Substorm Trigger Conditions

W. Horton, H. Vernon Wong, and J.W. Van Dam

Institute for Fusion Studies, The University of Texas at Austin

Austin, Texas 78712

March 23, 1999

Abstract

Critical conditions for the onset of fast interchange dynamics in the stressed geotail during the growth phase of the substorm are derived. We compare the ideal MHD interchange stability conditions (Hurricane, 1997) with kinetically modified interchange–ballooning motions. It is shown that fast interchange growth is possible only in the near–Earth boundary of the plasma sheet where the local plasma pressure is near unity since compressibility stabilizes the high beta geotail. The growth rate is proportional to the local current density and exceeds the ion bounce frequency in the local region of $\beta \lesssim 1$. Only after sufficient thinning of the current sheet will the kinetic theory growth rate exceed the bounce frequency of the ions which is the effective condition for the substorm MHD–space–time scale unloading of the plasma energy stored in geotail.

Keywords: 2736 Magnetospheric physics; Magnetosphere/ionosphere interactions 2744; Magnetotail 2752; MHD waves and instabilities 2788; Storms and substorms

1 Introduction

The stability of the geomagnetic tail has been discussed by Lee and Wolf (1992), Hurricane (1997), Bhattacharjee *et al.* (1998), and Lee (1998), using the ideal magnetohydrodynamic (MHD) equations. However, the geomagnetic tail plasma is collisionless, and a stability analysis based on the plasma kinetic equations rather than the plasma fluid equations would seem to be more appropriate. We reinvestigate the problem of interchange stability of the geomagnetic tail emphasizing the kinetic theory restrictions on the dynamics. Roux *et al.* (1991) describe the correlated measurements for particles and fields at GOES 2 during an isolated substorm with ground–based measurements of the westward traveling surge in the aurora to make the argument that the ballooning–interchange instability can account for several observed phenomena.

We deviate from the procedure in Lee and Wolf (1992) by not enforcing the vanishing compressibility condition obtained from the MHD minimization of the variational energy. This condition of zero plasma compression assumes that the parallel magneto–acoustic wave has sufficient time to establish the integral constraint on the trial function used by these authors. Here, we note that such a slow growth regime would be properly treated by the kinetic theory with a complex integral operator. In contrast, the regime of interest for the condition for substorm growth is a fast–growing regime in which there is no time for the system to establish the particular MHD constraint required by zero compression. This constraint is now replaced by the condition that the maximum growth rate $\gamma_{\max} > \omega_{bi}$ where ω_{bi} is the bounce frequency of the trapped ions. Here we show that shifting to this kinetic theory perspective on the stability problem changes the conclusions of Hurricane (1977) which is that the system is unstable for all regions where the plasma pressure satisfies

$$\beta > \frac{NL_pR_c}{L^2}$$

[his Eq. (25)] where L is the total length of the field line, $L_p = p/|\nabla p|$ the pressure gradient scale length, R_c is the minimum radius of curvature and N is a numerical factor which he estimates as $N \simeq 4 \times 10^4$. His conclusion is that for β larger than this critical β, the tail in the plasma is unstable. This would dictate that the entire geotail plasma is interchange unstable beyond and critical distance of about $10\,R_E$. We find a different result from the kinetic stability perspective. We find that there is only a region of $\beta \sim 1$ for instability in the near–Earthward edge of the central plasma sheet. For low β there is a threshold for instability that gives $\beta > \beta_1 \sim 0.2$ as shown, for example, in Fig. 4 of Lee (1998). For higher β there is a cut–off for $\beta > \beta_2$ for the fast–growing modes which we show are stabilized by plasma compressibility. While Hurricane may be technically correct that the high beta region is unstable to some residual, slow–growing modes, we feel that even here the final conclusion is not known until a kinetic stability theory analysis with an integral kernel over the complex orbits is performed.

Although we consider $\gamma_{\max} > \omega_{bi}$ for ions, the same is not necessarily the case for electrons. The electron bounce frequency may typically be faster than the unstable growth rates $\omega_{be} > \gamma_{\max}$, and the electron response should then be averaged over its trajectory. A proper kinetic stability theory analysis would then require the ion and electron response to be treated differently. This is a regime which is essentially not accessible in particle simulations where kinetic effects are investigated using low values of m_i/m_e since the separation between the ion and electron bounce frequencies may not be sufficient to be realistic.

For example, Pritchett *et al.* (1997) find for $m_i/m_e = 16$ and $T_e = T_i/4$ a weak interchange mode with $k_y\rho_i \cong 1$ for a monotonic $B_z(x)$ and a fast–growing mode for a nonmonotonic $B_z(x)$. They offer an explanation of the growth using the thermodynamic δW with the flux tube volume $V = \int ds/B$ and the field line length $L(\psi)$. Here ψ is the magnetic flux per unit length in the dawn–dusk direction $\hat{\mathbf{y}}$ such that $\mathbf{B} = \hat{\mathbf{y}} \times \nabla\psi$. The system is locally invariant in the y–direction. They propose that nonlinear saturation of the system occurs when the steepening of the gradients in the interchanged flux tubes becomes such that $k_\perp^{n\ell}\rho_i > 1$ so that ions average over both the Earthward and tailward fast flows set up by the interchange dynamics.

The focus of our investigation is the fast growth rate regime $\omega_{be} > \gamma > \omega_{bi}, \omega_i^*,\ \overline{\omega}_{di}$. We model the geotail with a relatively simple high beta equilibrium which enables us to evaluate analytically the field line integrals appearing in the stability analysis. We consider interchange modes with relatively long wavelength $k_\perp/k_\parallel \gg 1 \gg k_\perp \rho_i$ in the limit where parallel electric field perturbations can be ignored. Here ω_{be} and ω_{bi} are the bounce frequencies of the electrons and ions in the minimum B region, and ω_i^* and $\overline{\omega}_{di}$ are the ion diamagnetic drift frequency and the ion ∇B–curvature drift frequency in the strongly nonuniform magnetic field.

In the slow growth rate regime the kinetic theory effects are complicated by two issues (1) large ion gyroradius orbital chaos and (2) the existence of other trapped particle instabilities with electrostatic–like polarizations of the electric field. In a series of fundamental papers (Hurricane *et al.*, 1994, 1995a,b) investigate the stability of the MHD–like modes in with chaotic orbits. Only the case of strong chaos where it is possible to argue that the successive jumps in the magnetic moments are sufficient to isotropize the perturbed ion distribution functions are they able to proceed to a conclusion. In this strongly chaotic regime they show that for MHD–like assumptions with regard to the frequency and perpendicular wavelength the Bernstein *et al.* (1958) energy principle is recovered. Thus, they conclude that the stochastic plasma, as they call this regime in Hurricane *et al.* (1995b), is always less stable than a corresponding adiabatic (μ–conserving) plasma. Their final pressure perturbation is isotropic ($\delta p = \delta p_\perp = \delta p_\parallel$) and isothermal meaning that the effective value of the adiabatic gas constant Γ is unity. They give clear physical interpretations of these results for the case of sufficiently strong chaos in the ion orbits. We assume here that a small fraction of the thermal ion phase space is chaotic in the spatial region that is in the near–Earth geotail ($X \leq -10\, R_E$). We point to formulas of Delcourt and Belmont (1988) giving the limited phase space domain for significant variations of the magnetic moment in the near–Earth magnetotail.

On the second issue of non–MHD like polarizations we observe that for plasma beta near the onset of MHD–modes there are two modes (i) the kinetically modified MHD–modes with small $E_\|$ and (ii) the trapped particle modes with a significant $E_\|$. A detailed example for $\beta \sim \beta_1 \sim L_p R_c / L_\|^2$ is given in Hong *et al.* (1989) where the well–separated frequencies and polarizations of the two unstable modes are shown as a function of β/β_1. The electrostatic–like modes have a maximum growth rate near $k_\perp \rho_i \sim 1$ and produce a small scale turbulent diffusivity. The large scale kinetically modified MHD modes produce large scale plasma convection. Their growth rate maximizes at a low value of $k_y \rho_i$. The short wavelength trapped particle modes with finite parallel electric field perturbations have recently been discussed by Cheng and Lui (1998). We explore the effects of plasma compressibility on plasma stability as a function of plasma beta.

In Sec. 2 we begin our analysis of the variational energy released from fast growing MHD-scale perturbations using both the ideal MHD model and the Kruskal-Oberman kinetic theory formulation. We derive the critical dimensionless functions of plasma beta that define high beta stability due to the compressibility effects in plasma pressure and the magnetic field. We discuss the unstable window $\beta_1 < \beta < \beta_2$ for the growth of MHD space-time scale perturbations. In Sec. 3 we use the Tsyganenko (1996) magnetic field model and equliblrium force balance to calculate the pressure profile and show that the unstable region maps to the auroral arcs. We also use the Toffoletto *et al.* (1996) model to make the evaluation of the unstable region. In Sec. 4 we summarize our conclusions.

2 MHD and Kinetic Theory Energy Calculations

In the stretched magnetotail the curvature vector $\boldsymbol{\kappa} = \mathbf{b} \cdot \nabla \mathbf{b}$ of the field lines is large and sharply localized to the region where the magnetic field vector angle is closer to the

Northward direction than 45°. This region of large field line curvature is potentially unstable to interchange or ballooning instabilities which could release the locally stored plasma energy and disrupt the equilibrium configuration.

In this investigation, we explore the threshold for fast growing MHD instabilities using the plasma energy functional.

We consider two forms of the energy functional expressed in terms of the plasma displacement vector $\boldsymbol{\xi}$. The first form is the conventional MHD energy functional of Bernstein *et al.* (1958) and the second is the kinetic energy functional of Kruskal and Oberman (1958).

The plasma energy functional δW_p of Bernstein *et al.* (1958) can be written as follows

$$\delta W_p^{\mathrm{MHD}} = \frac{1}{2} \int \frac{d\psi dy ds}{B} \left\{ \gamma p_0 \left(\nabla \cdot \boldsymbol{\xi} \right)^2 + \left(\mathbf{Q}_\perp \right)^2 + \left(Q_L \right)^2 - 2\boldsymbol{\xi} \cdot \boldsymbol{\kappa} \boldsymbol{\xi} \cdot \nabla p_0 \right\} \tag{1}$$

where $\mathbf{Q}_\perp = \mathbf{b} \times (\mathbf{Q} \times \mathbf{b})$ is the perpendicular component of the perturbed magnetic field magnetic field $\mathbf{Q} = \nabla \times (\boldsymbol{\xi} \times \mathbf{B})$, and $Q_L = -B(\nabla \cdot \boldsymbol{\xi}_\perp + 2\boldsymbol{\xi} \cdot \boldsymbol{\kappa})$. The first term represents plasma compression, the second field line bending, the third magnetic field compression, and the fourth is the destabilizing term due to the pressure gradient. We assume zero parallel equilibrium currents due to the local dawn–dusk $\widehat{\mathbf{y}}$–symmetry. The plasma equilibrium is unstable if there exists a perturbation for which the minimum of $\delta W_p^{\mathrm{MHD}}$ is negative.

The displacement vector $\boldsymbol{\xi}$ has a parallel component $\xi_\| = \mathbf{b} \cdot \boldsymbol{\xi}$ which is present only in the plasma compression term. For slow growing instabilities where perturbations have sufficient time to propagate along the field line, plasma compression can be minimized by taking $\xi_\|$ to be the solution of the minimizing condition (Lee and Wolf, 1992)

$$\mathbf{B} \cdot \nabla \left(\nabla \cdot \boldsymbol{\xi} \right) = 0 \tag{2}$$

Thus plasma compression is constant along the field line and this effectively implies that

$$\nabla \cdot \boldsymbol{\xi} = \frac{\int \frac{ds}{B} \nabla \cdot \boldsymbol{\xi}_\perp}{\int \frac{ds}{B}}$$

where $\int \frac{ds}{B}$ is the line integral along the field line.

On the other hand, for fast growing instabilities in which there is insufficient time for plasma perturbations to relax along the field line, the condition should be $\xi_\parallel = \mathbf{b}\cdot\boldsymbol{\xi} = 0$. This limit is the focus of our investigation and we impose this condition in our analysis.

Thus we compute here

$$\delta W^{\mathrm{MHD}}(\xi_\parallel = 0) > \min_{\xi_\parallel}\left[\delta W^{\mathrm{MHD}}\right] \tag{3}$$

and show that $\delta W^{\mathrm{MHD}}(\xi_\parallel = 0) < 0$ for a certain range of β. Although our trial functions $\boldsymbol{\xi}_\perp$ is not the worst case trial function for strict MHD theory, they are the appropriate perturbations in the kinetic energy functional of Kruskal and Oberman in the limit of $\mathbf{b}\cdot\widetilde{\mathbf{E}} = 0$ where $\widetilde{\mathbf{E}}$ is the perturbed electric field.

We take the displacement vector $\boldsymbol{\xi}$ to be $\boldsymbol{\xi} = \mathbf{b}\times\widetilde{\mathbf{A}}_\perp/B$, where the perpendicular component of the perturbed magnetic potential $\widetilde{\mathbf{A}}_\perp$ is of the form

$$\widetilde{\mathbf{A}} = \widetilde{A}_\psi \nabla\psi + B\nabla_\perp \frac{\widetilde{\phi}}{B}$$

Thus

$$\boldsymbol{\xi} = \mathbf{b}\times\nabla\frac{\widetilde{\phi}}{B} + \widetilde{C}\widehat{\mathbf{y}} \tag{4}$$

where $\widetilde{C} = -\widetilde{A}_\psi$. Such perturbations reflect the dominant $\widetilde{\mathbf{E}}_\perp\times\mathbf{B}$ plasma motion in a strong magnetic field, where $\widetilde{\mathbf{E}}_\perp = -\frac{1}{c}\frac{\partial\widetilde{\mathbf{A}}}{\partial t}$.

The field variable $\widetilde{\phi}$ describes the field line displacement and $\widetilde{C}$ the magnetic field compression. Let $\xi^\psi = \boldsymbol{\xi}\cdot\nabla\psi = ik_y\widetilde{\phi}$, where the y–dependence of the perturbation is exponential $\sim \exp(ik_y y)$. Then we have from a series of calculations that

$$\boldsymbol{\xi}\cdot\boldsymbol{\kappa} = \frac{\boldsymbol{\kappa}\cdot\nabla\psi}{B^2}\xi^\psi$$

$$\nabla\cdot\boldsymbol{\xi} = -\boldsymbol{\xi}\cdot\boldsymbol{\kappa} + ik_y\widetilde{C}$$

$$\boldsymbol{\xi} \cdot \nabla p_0 = \xi^\psi \frac{\partial p_0}{\partial \psi} \tag{5}$$

$$\mathbf{Q}_\perp = i k_y \frac{\partial \widetilde{\phi}}{\partial s} \mathbf{b} \times \widehat{\mathbf{y}} + \mathcal{O}\left(\frac{\kappa}{k_y}\right)$$

$$Q_L = -\frac{\boldsymbol{\kappa} \cdot \nabla \psi}{B} \xi^\psi - i k_y B \widetilde{C}.$$

Minimizing $\delta W_p^{\rm MHD}$ [Eq. (1)] with respect to $\widetilde{C}$, we obtain in the limit of $|B^2 k_y^2 \widetilde{C}| \gg |B \frac{\partial}{\partial s} B \frac{\partial \widetilde{C}}{\partial s}|$ the polarization of the most unstable perturbation

$$\widetilde{C} = \frac{\gamma\beta - 2}{2 + \gamma\beta} \frac{\boldsymbol{\kappa} \cdot \nabla \psi}{B^2} \widetilde{\phi} \tag{6}$$

$$\beta = \frac{2 \mu_0 p_0}{B^2}. \tag{7}$$

After substituting Eq. (6) for $\widetilde{C}$ in Eq. (1), we have

$$\delta W_p^{\rm MHD} = \int \frac{d\psi dy ds}{B} \left\{ k_y^2 \left(\frac{\partial \widetilde{\phi}}{\partial s}\right)^2 + k_y^2 \frac{4\gamma\beta}{2 + \gamma\beta} \frac{(\boldsymbol{\kappa} \cdot \nabla\psi)^2}{B^2} \widetilde{\phi}^2 - 2 k_y^2 \frac{\boldsymbol{\kappa} \cdot \nabla \psi}{B^2} \frac{\partial p_0}{\partial \psi} \widetilde{\phi}^2 \right\}. \tag{8}$$

We now compare this MHD functional to the kinetic energy functional δW_p^K of Kruskal and Oberman which can be written as follows

$$\delta W_p^K = \frac{1}{2} \int \frac{d\psi dy ds}{B} \Big\{ (\mathbf{Q}_\perp)^2 + (Q_L)^2 - 2 \boldsymbol{\xi} \cdot \boldsymbol{\kappa} \boldsymbol{\xi} \cdot \nabla p_0$$

$$- \sum \int d^3 v \frac{\partial F_0}{\partial H_0} |\langle \mu Q_L + \boldsymbol{\xi} \cdot \boldsymbol{\kappa} (2 H_0 - \mu B) \rangle|^2 \Big\} \tag{9}$$

where F_0 is the equilibrium particle distribution function assumed to be isotropic, H_0 the particle kinetic energy, μ the particle magnetic moment, and the summation is over particle species. In writing Eq. (9) it is assumed that the frequencies ω of interest are larger than the plasma diamagnetic frequency ω^* and the particle drift frequency ω_D. The bracket $\langle (\cdots) \rangle$ is defined to be

$$\langle (\cdots) \rangle = \frac{\int \frac{ds}{v_\parallel} (\cdots)}{\int \frac{ds}{v_\parallel}} \tag{10}$$

where the integral is taken along a field line over a particle trajectory with constant H_0, μ.

In the limit where the frequency ω is also larger than the particle 'bounce' frequency ω_b along a field line, the calculation of δW_p^K can be simplified by evaluating the particle response locally, while in the opposite limit $\omega < \omega_b$, the particle response must be averaged over the particle "bounce" trajectory. However, to make our analysis tractable, we consider the ion pressure to be larger than the electron pressure ($p_i > p_e$), and we initially ignore the electron response. Later we treat the electron kinetic response perturbatively and we estimate its additional stabilizing effect. We defer a discussion of the more difficult case of $\omega \leq \omega^*, \omega_D, \omega_b$ and of anisotropic particle distributions.

Minimizing Eq. (9) with respect to Q_L as above, we obtain:

$$Q_L = -\boldsymbol{\xi} \cdot \boldsymbol{\kappa} \frac{3B}{2} \frac{\beta_i}{1+\beta_i} \tag{11}$$

and substituting Q_L in Eq. (9), we have

$$\delta W_p^K = \int \frac{d\psi dy ds}{B} \left\{ k_y^2 \left(\frac{\partial \widetilde{\phi}}{\partial s} \right)^2 + \frac{k_y^2 \beta_i}{2} \frac{7 + \frac{5}{2}\beta_i}{1+\beta_i} \frac{(\boldsymbol{\kappa} \cdot \nabla\psi)^2}{B^2} \widetilde{\phi}^2 - 2k_y^2 \frac{\boldsymbol{\kappa} \cdot \nabla\psi}{B^2} \frac{\partial p_0}{\partial \psi} \widetilde{\phi}^2 \right\}. \tag{12}$$

The plasma equilibrium is unstable if there are perturbations for which $\delta W_p^K < 0$ is negative and the magnitude of the destabilizing term proportional to the pressure gradient exceeds the sum of the stabilizing terms due to field line bending and plasma compression.

If we compare kinetic energy functional Eq. (12) with the MHD energy functional Eq. (8), we see that the energy released by the interchange force are similar but the kinetic calculation eliminates the unknown adiabatic gas parameter γ and changes the form of the compressional stabilization term.

To assess the relative magnitudes of these terms, we consider the standard local model of the high beta plasma equilibrium with a constant pressure gradient.

For the core of the central plasma sheet $dp/d\psi$ is constant and the solution of the Grad–Shafranov equation is

$$\psi = \frac{B_x' z^2}{2} - B_n x \tag{13}$$

where $\mathbf{B} = \hat{\mathbf{y}} \times \nabla\psi$ and $\nabla^2\psi = B'_x = \mu_0\, j_y = -\mu_0\, dp/d\psi$. In this region component of the curvature vector is strongly localized and given by

$$\boldsymbol{\kappa} = -\frac{\nabla\psi\, B_n^2 B'_x}{B^4}. \tag{14}$$

Substituting for $\boldsymbol{\kappa}$, we obtain from Eq. (14)

$$\delta W_p^{\mathrm{MHD}} = \int d\psi dy \left\{ k_y^2 \int \frac{ds}{B} \left(\frac{\partial\tilde{\phi}}{\partial s}\right)^2 - 2\frac{k_y^2\, {B'_x}^2}{{B_n}^2} \int \frac{ds}{B}\, \frac{B_n^4}{B^4} \tilde{\phi}^2 \left(1 - f(\beta_0)\right) \right\} \tag{15}$$

where $f(\beta_0) = f_1(\beta_0)$ and

$$f_1(\beta_0) = 2\gamma\beta_0 \int \frac{ds}{B}\, \frac{B_n^8}{B^8}\, \frac{\tilde{\phi}^2}{2 + \gamma\beta_0\, \frac{B_n^2}{B^2}} \Big/ \int \frac{ds}{B}\, \frac{B_n^4}{B^4}\, \tilde{\phi}^2 \tag{16}$$

$$\beta_0 = \frac{2\mu_0 p_0}{B_n^2}.$$

Since $ds/B = dz/B_n$ and $B = B_n(1 + z^2/L_z^2)^{1/2}$, we can readily evaluate the line integrals along the field line. We consider flute perturbations which minimize field line bending and we explore the stabilizing compressional effects with increasing plasma beta. For perturbations $\partial\tilde{\phi}/\partial s = 0$, we have the limiting values

$$f_1(\beta_0) \to \frac{5}{8}\,\gamma\beta_0 \qquad \beta_0 \to 0$$

$$f_1(\beta_0) \to 1.5 \qquad \beta_0 \to \infty.$$

The function $f_1(\beta_0)$ is plotted as a function of β_0 in Fig. 1. The fast MHD dynamics is stable for $\gamma\beta_0 > 5$.

From the kinetic energy functional Eq. (12), we obtain an expression similar to Eq. (16), but with $f(\beta_0) = f_2(\beta_{0i})$ where

$$f_2(\beta_{0i}) = \frac{7\beta_{0i}}{4} \int \frac{ds}{B}\, \frac{B_n^8}{B^8} \left(\frac{1 + \frac{5}{14}\,\beta_{0i}\frac{B_n^2}{B^2}}{1 + \beta_{0i}\frac{B_n^2}{B^2}} \right) \tilde{\phi}^2 \Big/ \int \frac{ds}{B}\, \frac{B_n^4}{B^4}\, \tilde{\phi}^2. \tag{17}$$

For perturbations $\partial\tilde{\phi}/\partial s = 0$, we have the limiting values

$$\begin{aligned} f_2(\beta_{0i}) &\to \frac{35}{32}\,\beta_{0i} \qquad \beta_{0i} \to 0 \\ f_2(\beta_{0i}) &\to \frac{25}{64}\,\beta_{0i} \qquad \beta_{0i} \to \infty. \end{aligned} \tag{18}$$

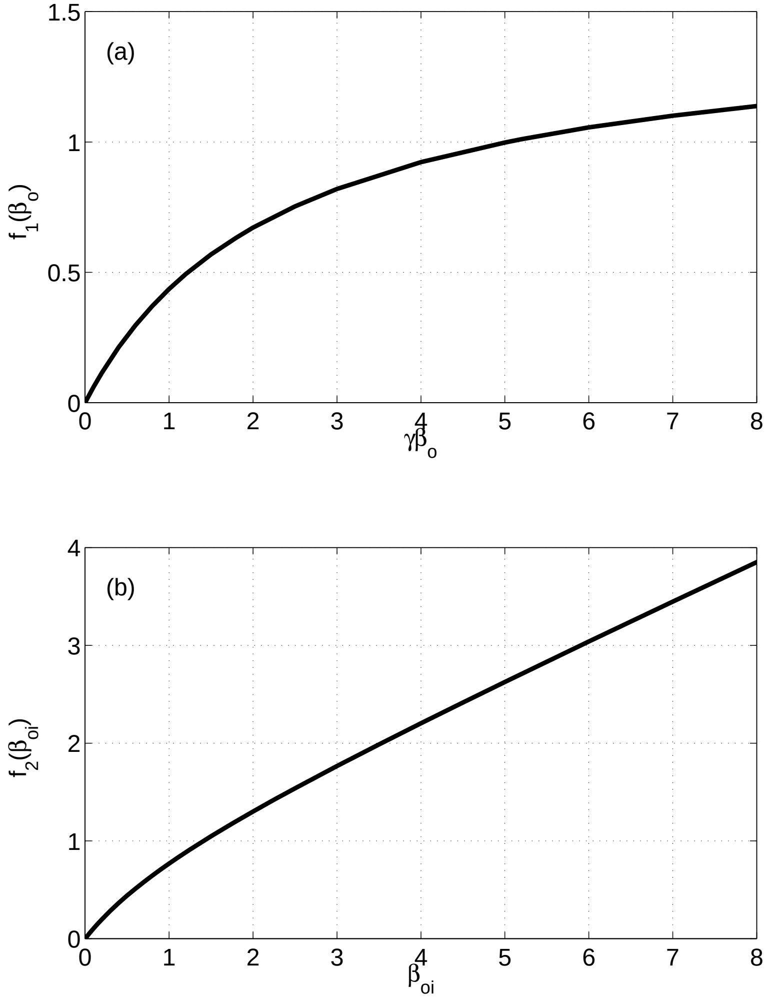

Figure 1: The critical function $f(\beta)$ defined such that $f = 1$ is the threshold for stability to fast interchange. (a) The MHD critical function $f_1(\gamma)$ defined in Eq. (16); (b) The kinetic theory critical function $f_2(\beta_i)$ defined in Eq. (17).

Note that at low values of $\beta_{0i} \leq 1$ the effective value of γ is $\gamma_{\rm kin} = 7/4$ as compared to $\gamma = 5/3$ in MHD.

Non-flute perturbations $\partial\widetilde{\phi}/\partial s \neq 0$ introduce an additional stabilizing effect of field line bending. However, if we ignore stabilization due to compressibility, we find that the most unstable perturbation is localized (ballooning) in the neighborhood of large curvature with an approximate field line variation $\widetilde{\phi} \sim (B_n/B)^n$, where the exponent is ~ 3.

We now considered the kinetic contribution of the electrons to the functional δW_p^K.

The full analysis of the electron bounce averaged contribution requires solving an integral–differential equation. Here we analyze the equation perturbatively using $T_e/T_i \ll 1$. We include this contribution perturbatively. Thus we obtain the electron contribution by substituting Eq. (11) for Q_L in calculating the electron response. The energy functional is then modified as follows:

$$\delta W_p^K = \delta W_p^{K(i)} + \delta W_p^{K(e)}$$

where $\delta W_p^{K(i)}$ is given by Eq. (12) and the electron kinetic contribution $\delta W_p^{K(e)}$ is

$$\begin{aligned}
\delta W_p^{K(e)} &= \frac{1}{2}\int \frac{d\psi dy ds}{B}\int d^3v\,\frac{F_{0e}}{T_e}|\langle \mu Q_L + \boldsymbol{\xi}\cdot\boldsymbol{\kappa}(2H_0 - \mu B)\rangle|^2 \\
&= \frac{1}{2}\int \frac{d\psi dy ds}{B}\int d^3v\,\frac{F_{0e}}{T_e}\left|\left\langle \boldsymbol{\xi}\cdot\boldsymbol{\kappa}\left\{2H_0 - \mu B\frac{(1+5\beta_i/2)}{(1+\beta_i)}\right\}\right\rangle\right|^2 \\
&= \int d\psi dy \frac{15 p_{0e}}{8}\int \frac{ds}{B_n}\int_0^{\frac{B_n}{B}} \frac{d\lambda}{(1-\lambda B/B_n)^{1/2}}\left\langle \frac{(\boldsymbol{\kappa}\cdot\nabla\psi)}{B^2}k_y\widetilde{\phi}\left\{2 - \lambda\frac{B}{B_n}\frac{(1+5\beta_i/2)}{(1+\beta_i)}\right\}\right\rangle^2
\end{aligned}$$

where the integration variable $\lambda = \frac{\mu B_n}{H_0}$ is the pitch angle.

We see that $\delta W_p^{K(e)} > 0$ and is proportional to the electron beta $\beta_e = 2\mu_o p_e/B^2$. The electron contribution adds to the stabilizing effect of compressibility discussed earlier.

Thus, we conclude that compressional effects will stabilize perturbations with growth rates exceeding the ion bounce frequency for $\beta > 1.5 - 3.0$. We have not yet analyzed in detail the low bounce frequency limit where the kinetic response in δW_p^K must be evaluated by averaging over the particle bounce trajectory. It may however be verified that, in this limit, a lower bound on δW_p^K is obtained by evaluating δW^{MHD} subject to the minimizing condition $\mathbf{B}\cdot\nabla(\nabla\cdot\boldsymbol{\xi}) = 0$ and replacing γ by unity.

3 Time Scale of the Ballooning Interchange Dynamics

The magnitude of the linear growth rates is given by

$$\omega^2 = 2\left[\frac{\delta W_p^{\mathrm{MHD}}}{\int \frac{d\psi dy ds}{B} m_i n_i (\boldsymbol{\xi}\cdot\boldsymbol{\xi})}\right]_{\min}.$$

This quadratic form is a variational form of the linearized MHD equation.

The Euler equation for the parallel component $\xi_\parallel = \mathbf{b}\cdot\boldsymbol{\xi}$ is:

$$n_i m_i \omega^2 \xi_\parallel = -\gamma p_0 \mathbf{b}\cdot\nabla\left(\nabla\cdot\boldsymbol{\xi}_\perp + B\mathbf{b}\cdot\nabla\frac{\xi_\parallel}{B}\right).$$

In the limit of $\omega^2\xi_\parallel \ll \frac{\gamma p_0}{n_i m_i}|(\mathbf{b}\cdot\nabla)^2\xi_\parallel|$ where typical growth times are longer than that for sound wave propagation along the field lines, plasma compression is constant along the field lines $\gamma p_0 \mathbf{b}\cdot\nabla\left(\nabla\cdot\boldsymbol{\xi}_\perp + B\mathbf{b}\cdot\nabla\frac{\xi_\parallel}{B}\right) = 0$. In the opposite limit of short growth times $\omega^2\xi_\parallel \gg \frac{\gamma p_0}{n_i m_i}|(\mathbf{b}\cdot\nabla)^2\xi_\parallel|$, it is appropriate to take $\xi_\parallel \to 0$.

Thus for fast growing instabilities ($\xi_\parallel = 0$), the linear growth rate is approximately given by

$$\omega^2 = -\left[\frac{\frac{2(B_x')^2}{B_n^2}\int \frac{ds}{B}\frac{B_n^4}{B^4}|\xi^\psi|^2\left(1-f(\beta_0)\right)}{\int \frac{ds}{B}\frac{m_i n_i}{B^2}|\xi^\psi|^2}\right]_{\min}.$$

The maximum value of the curvature is $|\boldsymbol{\kappa}|_{\max} = |B_x'|/B_n \equiv 1/R_c$ and is localized spatially over a distance Δz in the z-coordinate ($\Delta z \ll L_z$). We take the density n_i and $|\xi^\psi|^2$ to be constant in carrying out the field line integration and we approximate the growth rate for $\beta_0 < 1$ by

$$\omega^2 = -\frac{(B_x')^2}{\mu_0 m_i n_i}\left(1-f(\beta_0)\right) \tag{19}$$

Note that for the kinetic energy functional, we have $f = f_2(\beta_0)$ from Eq. (17) with limits (18).

From Eq. (19) we see that the high beta region is stable to fast ballooning interchange motion within both the compressible MHD description and the kinetic description. Thus, the high-beta geotail region, where $\mu p_0/B_n^2 > \beta_2$, is predicted to be stable due to plasma compressibility (The precise value of β_2 is given by $f(\beta_2) = 1.$). We therefore expect fast growing instabilities, which we will argue could serve as substorm triggers, to occur at the near-Earth edge of the central plasma sheet where the transition between the stretched field B_n joins to the geodipole field $B_{dp,z}$ and the plasma beta decreases to unity. We now use the Tsyganenko–96 model to show that this is in the region between $x = -6$ to $-10\,R_E$ where. $B_{dp} \sim 50$ to $100\,\mathrm{nT}$. We also use the Toffoletto–Hill–Ding (Ding, 1995) model to obtain a similar range $x = -5$ to $-8\,R_E$ for the plasma beta to equal unity.

The stability criterion and the growth rates are evaluated using the Tsyganenko–96 model. Figure 2 shows the geotail condition for the solar wind conditions of dynamic pressure $p_{\mathrm{dyn}} = 3nPa, |B_{\mathrm{IMF}}| = 10\,\mathrm{nT}$ and the $D_{\mathrm{st}} = -50\,\mathrm{nT}$ for two clock angles. The axial magnetic field $B_n(x,0,0)$ is shown in frame (a). The current density along the mid–plane $j_y(x,0,0)$ is shown in frame (b). The integration of the force balance equation $j_y B_z = dp/dx$ yields the pressure profile $p(x,0,0)$ shown in frame (c). In addition we integrate $\psi = \int^x B_z dx'$ to obtain the magnetic flux $\psi(x)$ per unit length (per meter) along the geotail axis. From this information we construct the $p(\psi)$ and $j_y(\psi)$ functions shown in Fig. 3.

We see that the $p(\psi)$ is roughly linearly increasing with ψ in the region beyond $X = -10\,R_E$. Since the interchange stability analysis is a local calculation the stronger variation of $p(\psi)$ in the near–Earth region does not appreciably change the results given here. In Fig. 4 we show the dimensionless plasma pressure, defined in Eq. (7), as function of distance down the tail. For all solar wind conditions the β profile in region beyond $X = -25$ is very high $\beta \gtrsim 100$. Thus the deep tail is always stable to the fast growing compressible modes. There may exist slow growing kinetic modes in the tail as the Hurricane instability condition suggests. The region of the vacuum dipolar field is seen to be closer to the Earth than the geosynchronous orbit position at $X \cong -6.6\,R_E$. In the region between $X = -6\,R_E$ to $-8\,R_E$ we see that the condition for fast ballooning interchange instability on the dimensionless

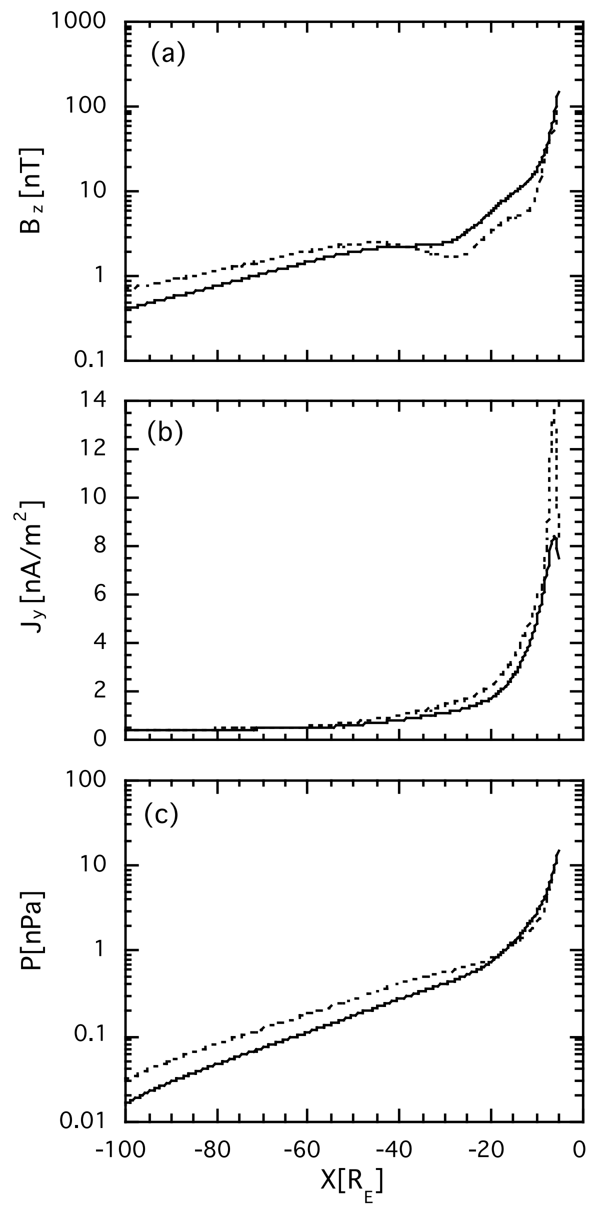

Figure 2: The profile of (a) $B_z(x,0,0)$, (b) $j_y(x,0,0)$, and (c) the associated pressure profile $p(x,0,0)$ required for (isotropic) force balance for the Tsyganenko (1996) model with $p_{\rm dyn}=3$, and $D_{\rm st}=-50$. The solid line is for the northward IMF with $B_z=10$nT and the dashed line is for a southward IMF with $B_z=-10\,$nT.

plasma pressure is fulfilled.

Now we consider the growth rate and the ion bounce frequency condition. We argue that the trigger condition is that the local current density $j_y \cong (dB_x/dz)\mu_0^{-1}$ in this near–Earth

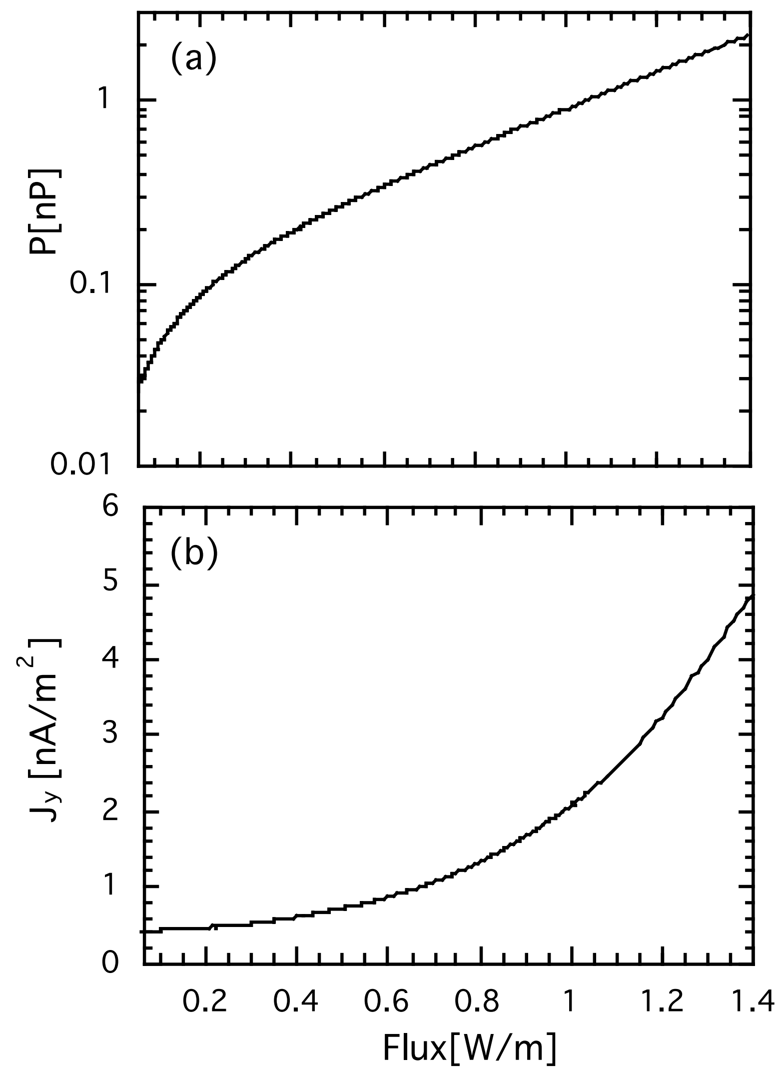

Figure 3: (a) The pressure $p(\psi)$ and (b) $j_y(\psi)$ obtained from Fig. 1 by integrating the flux equation $d\psi/dx = B_z(x,0,0)L_y$ with a fixed $L_y = 20\,R_E$ and the force equation $dp/dx = j_y B_z$. The pressure $p(\psi)$ and $j_y(\psi)$ functions are approximately linear in ψ ($dp/d\psi \cong \mathrm{const}$) for the region $-50\,R_E \leq x \leq -10\,R_E$.

region must increase to where Eq. (19) yields a growth rate $\gamma_{\max} \propto |j_y|$ greater than the ion bounce frequency $\omega_{bi} = 1/\tau_{bi}$ where

$$\tau_{bi}(v,\alpha) = 4\int_0^{S_T} \frac{ds}{v_\parallel} \simeq \begin{cases} \dfrac{2\pi\sqrt{2}R_c}{v} & \alpha > 1.0 \\[2ex] \dfrac{8\pi}{3}\,\dfrac{R_c}{v\alpha^3} & \alpha < 1.0 \end{cases} . \tag{20}$$

Here v is the particle speed and α is the pitch angle in radians. The ions with large pitch angles $\alpha > 1.0$ set the limit. From Eqs. (19) and (20) we derive the condition for the onset of fast ($\gamma > \omega_{bi}$), compressible MHD–like growth of the interchange modes

$$\gamma\tau_{bi} \cong 12.6 \left(1 - \frac{5}{4}\frac{\gamma\mu_0 p_0}{B_n^2}\right)^{1/2} \tag{21}$$

and

$$\frac{\partial B_x}{\partial z} \gg \frac{\partial B_z}{\partial x}.$$

Thus it is the lowest finite beta region ($\beta \gg \beta_1 \sim L_p R_c/L_\|^2 \sim 0.2$) with a substantially stretched tail field that goes unstable with the strength of an MHD interchange motion. (We estimate that $\partial B_x/\partial z \simeq 2\partial B_z/\partial x$ is the critical condition for substantial tail stretching which is equivalent to $(2\mu_0/B_z^2)(dp/dx) = 1/R_c$ using $\nabla_\perp(B^2/2 + \mu_0 p) = B^2\kappa$).

The fact that the stability condition depends only on β_n arises from the strong localization of the interchange energy release to the core of the central plasma sheet. In the core region the gradient $dp/d\psi$ is taken essentially constant and is proportional to the $\mu_0\, j_y = dB_x/dz$ as is the maximum curvature vector $\kappa_{\max} = B_x'/B_n$. This explains why Eq. (19) has B_x' as the common factor in both the $dp/d\psi$ and γp terms, and thus only the ratio of $(5/4)\gamma\mu_0\, p_0/B_n^2 \to f_1(\beta_0)$ between the compressible stabilization and the pressure gradient–interchange driving term determines the stability. The same situation is found in the high beta cylindrical pinch with a $B_\theta(r)$ field. This dependence on $(5/8)\gamma\beta_n(x)$ for high beta stability is in sharp contrast to the interchange condition in the near–Earth low beta region where $V = \int ds/B \cong R/B_{dp} = V_1(R/R_E)^4$ from the dipole magnetic field. In this inner low beta region the Earthward pressure gradient must exceed $-d_R \ell n\, p > \gamma V'/V = 4\gamma/R$ for interchange instability which is only satisfied for $R > R_{\rm crit} \sim 6\, R_E$. Thus the two criteria obtained from the low beta interchange and the high beta ballooning modes show that the most susceptible region to the onset of interchange instability is the transition region between the dipolar field and the high beta plasma sheet. The relation between the classical low beta stability criterion $-p' > \gamma p V'/V$ and the finite beta interchange which involves the compressional perturbation $\delta B_\parallel$ is somewhat intricate. We explain this relationship in detail in the Appendix. Finally, we note that the rigid interchange of flux tubes is not dynamically accessible once the ionospheric conductivity is taken into account. Thus the dynamical modes are always ballooning interchange modes.

From the Tsyganenko–96 model shown in Fig. 4, we see that the onset of the interchange motion will onset at $-10\,R_E < X \leq -6\,R_E$ as the increase of $B_x' = \mu_0 j_y$ occurs during the growth phase of the substorm dynamics. After the current density j_y exceeds $j_{y,\mathrm{crit}} \sim \frac{\partial B_z}{\mu_0 \partial x}$ by a factor of 2 to 3 the critical value, the onset of rapid unloading of the plasma controlled by the nonlinear interchange dynamics as observed in the MHD simulations will follow. This conclusion appears consistent with the particle simulations of Pritchett *et al.* (1997).

For comparison we show the plasma pressure, axial B_z field and $\beta(x)$ in Fig. 5 obtained from the Toffoletto *et al.* model (Toffoletto *et al.*, 1996, and Hesse and Birn, 1993). The unstable region shifts Earthward by about $1\,R_E$ for this model.

Two recent simulations studies of substorm onset include the external driving electric field to produce a time–evolving equilibrium. In the MHD simulations Bhattacharjee *et al.* (1998) solves the local ballooning mode equation at a sequence of positions along the geotail at each time value in the simulation. They find that the position for the most negative value of δW^{MHD} with $\Gamma = 5/3$ and using the integral equation constraint on $\xi_\parallel$ given in Eq. (12) with ionospheric boundary conditions that $\xi = 0$ (line–tied) at the $s = \pm L$. They conclude that instability sets in when the current sheet has thinned sufficiently. Bhattacharjee compares the compressible case with the incompressible mode equation finding that the incompressible solution is always stable (We show that the compressible solutions are unstable in the inner edge of the plasma sheet where $\beta < 1$.). Bhattacharjee shows an example when a compressible eigenmode goes unstable at $X = -10\,R_E$ for a particular numerical simulation. We argue that the slow growing compressible, high beta instability reported by

Bhattacharjee requires kinetic theory. Thus, kinetic theory calculations and simulations are important for the substorm trigger issue.

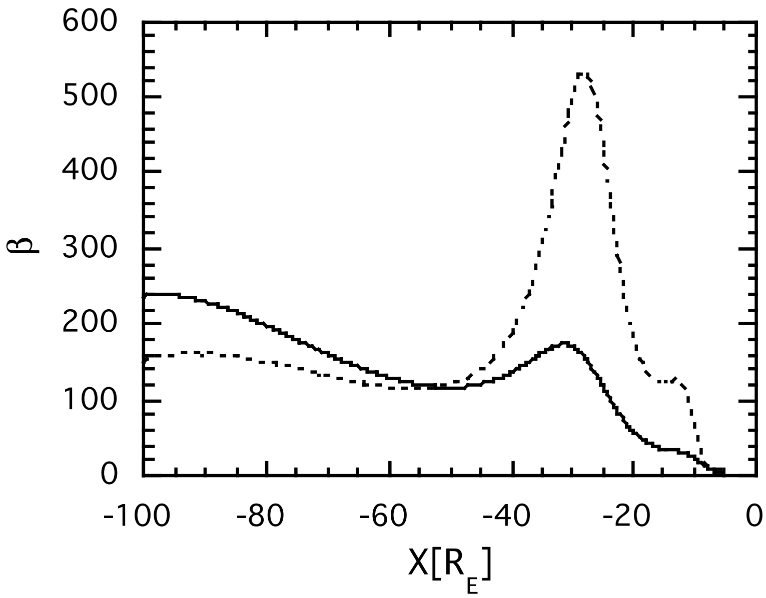

Figure 4: The dimensionless plasma pressure $\beta = 2\mu_0 p(x)/B_z^2(x)$ on the geotail axis in the region susceptible to interchange instability.

A conceptually similar setup is used by Pritchett *et al.* (1997) with 3D particle simulations. The system is bounded in X, Z with outflowing Neumann boundary conditions at the tailward end of the box and rigid Dirichlet conditions at the Earthward edge. Pritchett *et al.* find that an imposed large scale electric field produces an Earthward $\mathbf{E} \times \mathbf{B}$ convection of the plasma and a tailward convection of magnetic flux $\mathbf{v} \cdot \nabla\psi$. The system remains stable until the Earthward convection produces a negative $B_z(X, 0, 0)$ in the region near the Earthward boundary of the box where $B_z(-10, 0, 0) = 5.10 B_0$ with $\delta\mathbf{B} = 0$ on the boundary. When the convection drives $B_z(X, 0, t) < 0$ a ballooning–interchange mode grows localized in the region of anomalous dB_z/dx with the lowest $k_y = 2\pi/L_y$ in the box. The box size is $L_x L_y L_z = 100\Delta \times 128\Delta \times 192\Delta$ where $\Delta = 0.13\, R_E$ and the initial current sheet width is $L = 24\Delta = 4\rho_{i0}$. The mode appears and becomes strongly nonlinear in the time $\Delta t \Omega_{i0} \cong 60$. If we take $\gamma\Delta t = 10$ then $\gamma/\Omega_{i0} = 1/6$ for the simulation with $m_i/m_e = 16$ and $T_{i0}/T_{e0} = 4$.

The lowest k_y–mode in the box has $k_y\rho_i = 0.3$ suggesting that it requires a kinetic theory analysis as given here. The final time limitation to the simulation is stated to arise from the fact that the coupling to the ionosphere through parallel currents is not included.

Recently, Cheng and Lui (1998) considered a short wavelength $k_y\rho_i \sim 1$ trapped particle instability as a candidate instability for the substorm trigger. For these small space scale drift wave–trapped particle instabilities we would expect a turbulent thermal diffusivity rather than global MHD–like change in the pressure profile. Whether the small scale trapped particle modes can play an important role in the substorm is not yet clear.

We do expect that resonant fast ions that occur when the finite wave frequency $\omega \to \frac{1}{2}\,\omega_{*i} + i\gamma_k$ is included to be important. These kinetic ion resonances produce wave growth outside the beta window $\beta_1 < \beta < \beta_2$ given here. Thus the region just above β_2 will have slower growing resonant modes. Slow resistive damping sets in from increased coupling to the ionosphere for large scale modes, $k_y < k_y(\Sigma_p)$, where Σ_p is the Pedersen conductivity of the ionosphere.

4 Conclusions

The critical conditions for the onset of local interchange motions in the geomagnetic tail are reinvestigated with the distinction between fast, compressible motion and slow, incompressible motions emphasized. The MHD instability condition obtained by strict minimization of the MHD variational energy gives an incompressible displacement and the $\beta = 2\mu_0 p/B_N^2$ threshold as given, for example, by Hurricane (1997). We point out that such displacements require kinetic theory treatments for the bounce averaging of the particle response functions strongly modify the stability criterion. While slow growing kinetic instabilities may eventually be important, they need to be considered in the context of the 1 min fluctuations that occur in the plasma sheet. In addition, slow growing modes may saturate at a low level.

Here we evaluate both the MHD and the Kruskal–Oberman variational energy for fast,

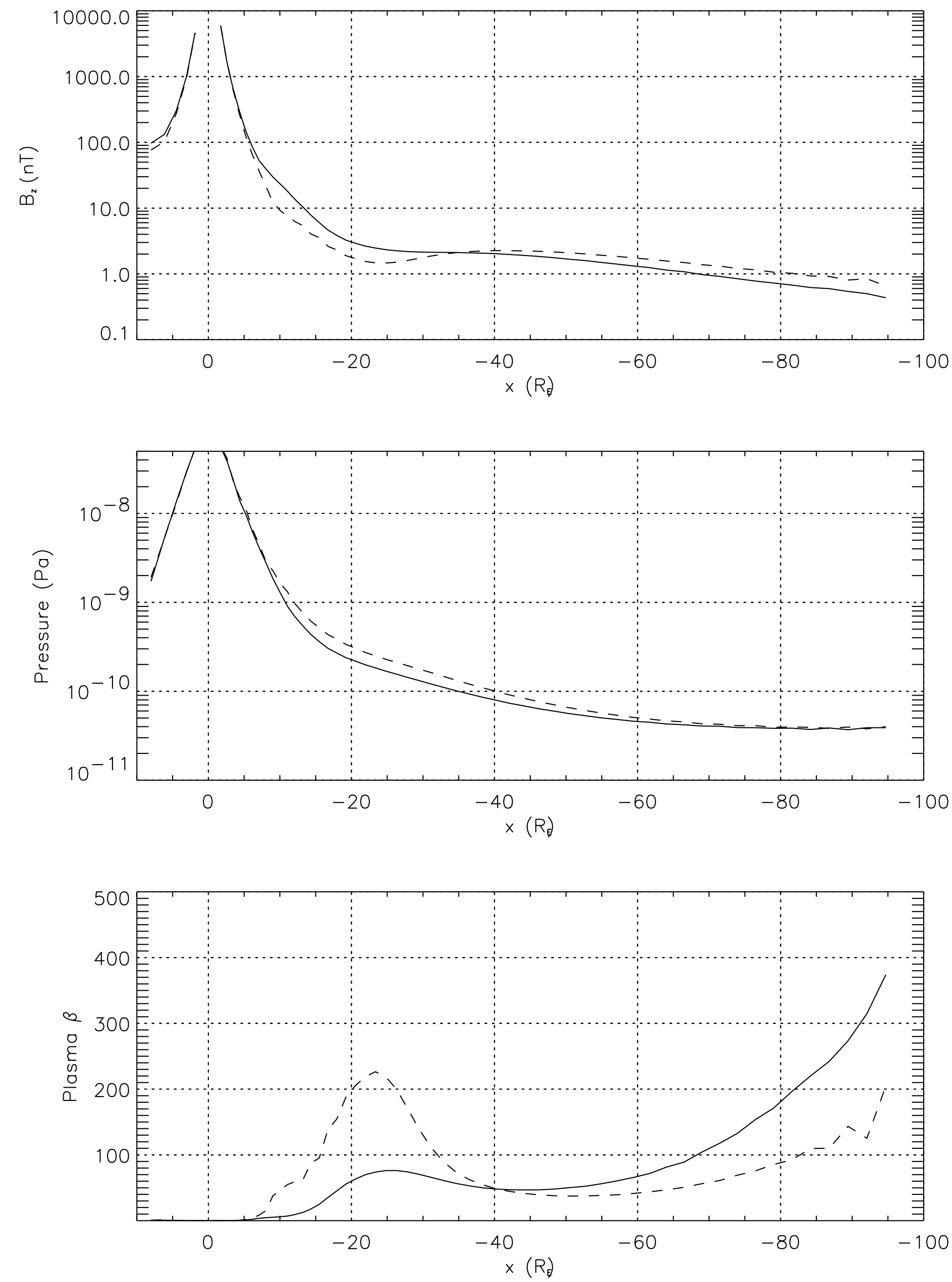

Figure 5: The profiles from Toffoletto *et al.* magnetospheric code. The solid line is for $B_z^{\rm IMF} = +10\,$nT and the dashed line for $B_z^{\rm IMF} = -10\,$nT. Top panel gives the B_z–field, the middle panel gives the plasma pressure on axis $(y = z = 0)$ and (c) the corresponding axial dimensionless plasma pressure $\beta(x)$.

compressible displacements. We argue that for the large–scale MHD–like energy releases the system must be unstable to the modes growing faster than the ion bounce time which is about 10s for deeply trapped ions. With this condition the trigger for the fast interchange is then that there be plasma with $\beta \lesssim 1$ in the near–Earth region $X = -6$ to $-10\, R_E$ with sufficient stretching of the magnetic field that $\mu_0 j_y = \partial B_x/\partial z > 2|\partial B_z/\partial x|$.

Clearly, the problem of determining precisely the location and the $|\partial B_x/\partial z|$ to $|\partial B_x/\partial z|$–ratio and plasma pressure and its gradient requires more detailed evaluations of the variation energy than given here. There also remains the question of the transitions from the fast, compressible modes to the slow, incompressible modes. These considerations, while complex and technically difficult, are not expected to change the picture of the interchange dynamics developed here with simpler considerations.

The lower limit on k_y is set by the requirement that the growth rate be faster than the ion bounce frequency. The physics determining the details of the minimum k_y is complicated due to the change of the eigenmode structure for large scale modes. The most severe limit comes from the slow resistive damping that sets in from increased coupling to the ionosphere for large scale modes. To take the ionospheric damping into account, the boundary condition on the ballooning mode equation brings in the height integrated Pedersen conductivity Σ_p. For sufficiently low k_y the growth rate is a significantly reduced by ionospheric damping of the perturbed parallel current.

The plasma beta region identified here by the stability analysis as being most susceptible to a fast MHD interchange growth maps to the auroral arc latitudes. This correspondence makes the hypothesis that the onset of the substorm is triggered by a fast MHD interchange–ballooning instability consistent with the visible and ultraviolet emission observations of Frank *et al.* (1998) that identify substorm onset as occurring on pre-existing auroral arcs. Frank *et al.* (1998) map the field lines to the inner edge of central plasma sheet placing the limits for the position $X_{\rm onset}$ for the initiation of the substorm as $-8\, R_E > X_{\rm onset} > -12\, R_E$.

Several minutes after the initial onset there is a rapid (explosive) spread poleward of the emission corresponding to a tailward expansion to $X = -20\,R_E$ to $-25\,R_E$. Frank *et al.* (1998) conclude that a trigger at $X = -8\,R_E$ to $-10\,R_E$ sets up the release of a large volume of plasma energy from the central plasma sheet.

Earlier auroral substorm observations and time correlated CCE spacecraft particle and field measurements lead Lui and Murphree (1998) to state that two observational constraints exist for a viable substorm onset theory. First, that the substorm expansion onset or trigger must reside on magnetic field lines threading an auroral arc. Secondly, that the near–Earth magnetic field must change from a tail–like configuration toward a more dipolar configuration. This requirement leads to the inference that there is a substantial diversion ($> 10^6$ A) of the cross–tail current instabilities (Lui *et al.*, 1993; Yoon and Lui, 1993) are argued to be viable models for the current diversion.

Acknowledgments

The authors thank C. Crabtree for the numerical work with the magnetic field models. This work was supported by the NSF Grant No. ATM-97262716 and the U.S. Department of Energy Contract No. DE-FG03-96ER-54346.

Table I: Space and Time Scales for Interchange Dynamics

Growth rate

$$\gamma_{\max} = \left(\frac{1}{\rho} \frac{dp}{dx} \frac{1}{R_c} \right)^{1/2}$$

$$\kappa_{\max} \equiv \frac{1}{R_c} = \frac{B'_x}{B_n}$$

Force balance $dp/dx = j_y \, B_n$ yields

$$\gamma_{\max} = |B'_x|/(\mu_0 \rho_0)^{1/2}$$

Deeply trapped ions

$$\omega_{bi} = \frac{v_i}{R_c}$$

Transient and weakly trapped ions

$$\omega_i = \frac{v_i}{L_z}$$

Parallel Transport and times

$$\tau_\parallel^i = \frac{L_\parallel}{v_i}$$

$$\tau_\parallel^e = \frac{L_\parallel}{v_e}$$

Diamagnetic drift velocity

$$v_{di} = \frac{cT_i}{eB_nL_{xp}}$$

Appendix: Interchange Instability Criteria in Low and High Plasma Pressure Limits

The analysis of the interchange instability in terms of an exchange of flux tubes leads to well–known thermodynamic stability conditions. One example is the case of a low pressure plasma (considered by Rosenbluth and Longmire, 1957), for which the magnetic tension is great. Then the most unstable interchange is one between tubes of equal flux, since the change in the magnetic field energy is zero. The change in energy is entirely given by the change in the plasma thermal potential energy:

$$\delta W = \delta W_p \cong \delta V \left(\delta p + \gamma p \, \frac{\delta V}{V} \right),$$

where δp is the pressure change, δV is the change in the volume $V = \int ds/B$ of the flux tube, and γ is the adiabatic index. Another case is that of an incompressible interchange between the two flux tubes of equal volume. Here, the plasma thermal energy does not change, and the change in the magnetic field energy is given by

$$\delta W_m = -\delta(\Phi^2) \frac{\delta(\ell^2)}{V}$$

where ℓ and Φ are the length and magnetic flux of the tube, respectively.

The most general type of interchange is one that preserves total pressure balance locally. This means that the volume of a displaced flux tube adjusts itself in response to both a different pressure and a different magnetic field strength in order to maintain total pressure balance inside and outside. For the sake of simplicity, consider a purely two–dimensional situation, so that the volume of the flux tube varies only in cross–section and hence $V \propto 1/B$. For this type of interchange (with $\delta\ell = 0$ and $\delta\Phi = 0$), the change in the total energy is given by

$$\delta W = \delta W_m + \delta W_p = \frac{pV(\delta p + B\delta B)\left(\dfrac{\delta B}{B} - \dfrac{\delta p}{2p} \right)}{(2p + B^2)}.$$

This stability condition reproduces precisely the condition derived by Bernstein *et al.* (1958) for an axisymmetric shearless system if we translate their quantities V' and L' as B^{-1} and B^{-3}, respectively, and use $\gamma = 2$. Also, it reduces to the low–beta interchange stability condition in that limit.

We now wish to show that the general interchange stability condition of the preceding paragraph is the same as that which we have derived for the substorm trigger problem. First, note that the pressure and magnetic field changes in the general interchange stability condition are the changes viewed in the moving frame of the displaced flux (i.e., the so–called Lagrangian changes), given as

$$\delta p = \delta p_L \equiv \delta p_E + \boldsymbol{\xi} \cdot \nabla p = -\gamma p \nabla \cdot \boldsymbol{\xi},$$

$$\delta B = B_{\parallel L} \equiv \delta B_{\parallel E} + \boldsymbol{\xi} \cdot \nabla B = -B(\nabla \cdot \boldsymbol{\xi}_{\perp} + \boldsymbol{\xi} \cdot \boldsymbol{\kappa}).$$

Second, recall that the Eulerian pressure and magnetic field changes are related through the quasistatic pressure balance condition $\delta p_E + B \delta B_{\parallel E} \cong 0$. The quasistatic results from the fact that the fast magnetosonic (compressional Alfvén) wave acts quickly to equalize the total transverse pressure. Now, if we use both of these pieces of information, we can rewrite the general interchange stability condition of the preceding paragraph in the following form:

$$\delta W = \frac{1}{2} V \frac{(\boldsymbol{\xi} \cdot \boldsymbol{\kappa})(\boldsymbol{\xi} \cdot \nabla p - 2p \boldsymbol{\xi} \cdot \boldsymbol{\kappa})}{\left(1 + \dfrac{2p}{B^2}\right)},$$

where, more generally, the factor V is replaced by a volume integration. We observe not only the usual destabilizing interchange term that involves the product of the curvature and the pressure gradient, but also a stabilizing term coming from the finite compression that involves the product of the curvature with itself. The latter effect is what causes the stability that we find in the substorm trigger problem when the plasma beta value exceeds approximately unity.

References

I.B. Bernstein, E.A. Frieman, M.D. Kruskal, and R.M. Kulsrud, Proc. Soc. (London) **A**244, 17 (1958).

A. Bhattacharjee, Z.W. Ma, and Xiaogang Wang, Ballooning instability of a thin current sheet in the high–Lundquist–number magnetotail, Geophys. Res. Lett. **25**, 861 (1998).

C.Z. Cheng and A.T.Y Lui, Lee, Kinetic ballooning instability for substorm onset and current disruption observed by AMPTE/CCE Geophys. Res. Lett. **25**, 4091 (1998).

D.C. Delcourt and G. Belmont, "Particle dynamics in the near–Earth magnetotail and macroscopic consequences," in *New Perspectives on the Earth's Magnetotail*, edited by A. Nishida, D.N. Baker, S.W.H. Cowley, (American Geophysical Union, Washington, DC, 1998), pp. 193–210.

C. Ding, Analytical and Numerical Modeling of the Electromagnetic Structure of Geospace, (Ph.D., Dept. of Space Physics/Astronomy, Rice Univ., April, 1995).

L.A. Frank, J.B. Sigwarth and W.R. Paterson, High–resolution global images of Earth's auroras during substorms, in *Substorms–4*, S. Kokubun and Y. Kamide, eds., pp. 3–8, Kluwer Academic Publishers, Dordrecht, The Netherlands (1998).

M. Hesse, and J. Birn, Three-dimensional magnetotail equilibria by numerical relaxation technique, J. Geophys. Res. **98**(A3), 3973–3982 (1993).

B.-G. Hong, W. Horton, D.-I. Choi, Pressure gradient-driven modes in finite beta toroidal plasmas, Plasma Phys. and Control. Fusion **31**, 1291 (1989).

W. Horton and I. Doxas, A low-dimensional energy conserving state space model for substorm dynamics, J. Geophys. Res. **101**, 27,223–27,237 (1996).

O.A. Hurricane, R. Pellat, and F.V. Coroniti, The kinetic response of a stochastic plasma to low frequency perturbations, Geophys. Res. Lett. **21**, 4,253 (1994).

O.A. Hurricane, R. Pellat, and F.V. Coroniti, The stability of a stochastic plasma with respect to low–frequency perturbations, Phys. Plasmas **2**, 289 (1995a).

O.A. Hurricane, R. Pellat, and F.V. Coroniti, A new approach to low–frequency "MHD–like" waves in magnetospheric plasmas, J. Geophys. Res. **100**, 19,421–19,428 (1995b).

O.A. Hurricane, R. Pellat, and F.V. Coroniti, Instability of the Lembége–Pellat equilibrium under ideal magnetohydrodynamics, Phys. Plasmas **3**, 2472 (1996).

O.A. Hurricane, MHD ballooning stability of a sheared plasma sheet, J. Geophys. Res. **102**, 19,903 (1997).

M.D. Kruskal and C.R. Oberman, Phys. Fluids **1**, 275 (1958).

D.–Y. Lee and R.A. Wolf, Is the Earth's magnetotail balloon unstable? J. Geophys. Res. **97**, 19,251–19,257 (1992).

D.-Y. Lee, Geophys. Res. Lett. **25**, 4095 (1998).

A.T.Y. Lui and J.S. Murphree, A substorm model with onset location tied to an auroral arc, J. Geophys. Res. **25** 1269–1272 (1998).

A.T.Y. Lui, *et al.*, Quasilinear analysis of ion Weibel instability in the Earth's neutral sheet, J. Geophys. Res. **98**, 153, 1993.

P.L. Pritchett and F.V. Coroniti, Interchange and kink modes in the near–Earth plasma sheet and their associated plasma flows, Geophys. Res. Lett. **24**, 2925–2928 (1997).

P.L. Pritchett, F.V. Coroniti, and R. Pellat, Connection–driven reconnection and the stability of the near–Earth plasma sheet, Geophys. Res. Lett. **24**, 873–876 (1997).

M.N. Rosenbluth and C.L. Longmire, Ann. Phys. (N.Y.) **1**, 120 (1957).

A. Roux, S. Perraut, P. Robert, A. Morane, A. Pedersen, A. Korth, G. Kremser, B. Aparicio, D. Rodgers, and R. Pellinen, Plasma sheet instability related to the westward traveling surge, J. Geophys. Res. **96**, 17,697–17,714 (1991).

F.R. Toffoletto, R.W. Spiro, R.A. Wolf, M. Hesse, and J. Birn, "Self-consistent modeling of inner magnetospheric convection," in *Third International Conference on Substorms (ICS-3)*, edited by E.J. Rolfe, and B. Kaldeich, (ESA Publications Division, Noordwijk, The Netherlands, 1996), pp. 223–230.

N.A. Tsyganenko, and D.P. Stern, Modeling of the global magnetic field of the large-scale Birkeland current systems, J. Geophys. Res. **101**, 27187–27198 (1996).

P.H. Yoon and A.T.Y. Lui, Nonlinear analysis of generalized cross–field current instability, Phys. Fluids B **5**(3), 836, 1993.